SPACE TELESCOPE SCIENCE INSTITUTE

INSTRUMENT SCIENCE REPORT

CAL/FOS-025

TITLE: FOS Linearity Corrections

AUTHOR: D. Lindler and R. Bohlin DATE: January 1986

ABSTRACT

Data taken during June and August 1984 show that the FOS diode non-linearity (paired pulse correction) can be modelled by:

$$x = \frac{y}{(1 - ty)} ,$$

where y is the observed count rate (counts/sec) and x is the true count rate. The time coefficient t is constant (9.43 microsec) up to 51,000 observed counts per sec, which corresponds to a true input rate of about 100,000. Above 51,000 counts t can be modelled by:

$$t = 9.43 \times 10^{-6} + 2.568 \times 10^{-10} (y - 51000)$$

This variation in t may be caused by photocathode "fatigue".

No significant diode to diode variation in the nonlinearity is seen below 100,000 true (input) counts/sec. Above this count rate the observed count rate varies from diode to diode by as much as ± 10%.

The accuracy of this model in predicting true corrected count rates should be better than 1% below 20,000 and degrading to about 5% for an average of many diodes at 100,000 true counts/sec.

The results presented here should be used only as a guide to the reduction of flight data, because the red tube has been replaced and the blue tube has not been studied at the highest counting rates. The fatigue effects may be quantitatively different for flight conditions.

DISTRIBUTION:

ISB

CSC

SDAS

SOGS

IDT

## I. Introduction

The FOS dectectors are two Digicons with 512 independent diodes and pulse counting channels. The counting circuitry of the detectors is not able to count all photoelectrons received. After recording a pulse from one event (electron) there is a recovery time before a second event can be detected. Photon arrivals are described by Poisson statistics. As the mean time interval between events decreases, a significant number of events will be separated by less than the recovery time. These "paired pulses" would be counted as a single event, causing the observed counting rate to be less than the actual rate of photoelectron events. As the mean interval becomes shorter than the recovery time, the detector would never recover and no counts would be recorded. To avoid this paralysis at very high counting rates, a "dead time" is built into the counting circuitry, which is chosen longer than the recovery time. After counting an event, the channel is turned off for one dead time interval.

An analytical model of the observed count rate as a function of the actual count rate may be derived as follows: let y be the observed count rate and t the dead time. For a time interval T the number of events counted will be Ty. The total time the circuit is "dead" is tTy. The total time the circuit is "alive" and can count events is T - tTy. If x is the actual rate of events the total number of events counted is given by (T - tTy)x. (The time the circuitry is enabled times the mean rate of events).

Therefore:

$$Ty = (T - tTy)x \qquad (1)$$

or equivalently:

$$x = \frac{y}{1 - ty} \qquad (2)$$

The FOS dead time is 10 clock pulses of 0.977 microsec from a 1.024 megahertz clock. Depending on when an event arrives, the dead time can vary from 9 x 0.977 or 8.79 microsec (if the event occurs immediately before a clock pulse) to 10 x 0.977 or 9.77 microsec (if the event occurs immediately after a clock pulse).

## II. Data

The non-linearities in the counting rates were measured by holding the light output from the optical simulator constant while changing the light input to the FOS detectors by known amounts. The light input to the detectors was varied by selection of different entrance apertures.

Data were taken in August 1984 using the ambient ST optical simulator with a tungsten lamp. Grating H57 on the red tube and grating H40 on the blue tube were used. For each detector, data were taken for all entrance apertures. For the blue tube, observed counting rates varied from less than 100 counts/sec

(aperture A4, 0".1 square) to approximately 50,000 (aperture A1, 4".3 square). Count rates for the red tube varied from less than 1000 counts/sec (A4) to 70,000 counts/sec (A1). Observations were repeated for all apertures with a 10% neutral density filter inserted to decrease the input count rate by approximately a factor of 10, in order to compute the relative aperture sizes. Because of the decreased count rates, the neutral density filter minimized the effect of the nonlinearity on the aperture size computations.

All data were taken with no overscanning to allow analysis of diode to diode variations. Exposure times were computed to accumulate over 100,000 total counts, making counting statistic errors negligible in the analysis.

To avoid filter/grating wheel repeatability problems, all data for each detector was taken without moving the grating wheel. Y-bases were checked and adjusted immediately prior to taking the blue tube data to minimize the effects of spectral motion due to thermal changes and high voltage settling. This check was not done for the red tube.

## III. Data Reduction

The first step in the data analysis was to determine the relative aperture sizes versus diode number (or equivalently, wavelength). Blue side data taken with the 10% neutral density filter were corrected for non-linearities using a preliminary paired-pulse model (E. Beaver, Private Communication). Since count rates were small (<10,000 counts/sec), errors resulting from inaccuracies in the model were not significant. Aperture sizes relative to the B1 (0.5 arcsec circle) were computed for each diode by dividing the corrected count rate of all apertures by the corrected count rate of the B1 aperture. Because of significant diffraction losses for the smaller apertures that cause the ratios to vary as a function of wavelength, a linear fit to each ratio versus diode number was used as the relative aperture size.

The second step was to compute the true count rate for each aperture when the neutral density filter was not in place. The B1 aperture was used as a reference. The data for the B1 aperture were corrected with the preliminary paired pulse model. (Errors were not significant because of the small count rate, <2200 counts/sec). The expected count rate for the other apertures was then computed for each diode by multiplying the corrected B1 spectra by the relative aperture sizes. Using data from all apertures, a table of true counts, x, versus observed counts, y, was created. For each data point, a dead time was computed by:

$$t = \frac{1}{y} - \frac{1}{x} \quad , \qquad (3)$$

which is equation (2) solved for t.

## IV. Analysis

The time constant versus observed count rate was first computed for the blue tube. The results are plotted in Figure 1. The scatter in the data is mostly attributed to photocathode granularity (see secion V). At low count rates, small deviations in the expected count rate results in a large error in the computed time constant. An average time constant of 9.43 microsec was computed using data above 30,000 counts/sec. This region has the least scatter and is where an accurate time constant is most critical for removal of non-linearity.

Figure 2 shows a plot of the observed count rate versus the true count rate for all data points. Overplotted with a solid line, is the non-linearity model with t=9.43 microsec.

The time constant of t=9.43 microsec is in agreement with the built-in dead time of 10 clock pulses of a 1.024 megahertz clock. Depending on when a pulse arrived the dead time could vary from 8.79 microsec to 9.77 microsec with an average of about 9.3 microsec.

The analysis was repeated for the red side. The plot of time constant versus y is shown in Figure 3. Three anomalies are evident. An apparent variation of the time constant from one side of the diode array to the other is evident for some of the apertures, as seen by the curved structure of the data between 30,000 and 50,000 counts/sec. The second anamoly is a significant increase in the time constant above 50,000 counts/sec. The third anomaly is the increased scatter of the data points around 60,000 counts/sec. As stated previously, the scatter should be smaller at higher count rates.

The increased time constant above 50,000 counts may be due to photocathode fatigue. Figure 4 shows a plot of the spectra from all apertures versus diode number. The central part of the aperture C3 (2 x 2 arcsec with occulting bar) shows a flattening of the spectrum with a slight dip in the center, which suggests that the fatigue in the center of the photocathode is greater than at the sides. The spectrum for the A1 aperture begins to show the correct curvature indicating that fatigue also becomes prominent at the edges at higher count rates. A second possibility for the flattening of the C3 spectrum is a y-base that is in error by about 40 microns, causing part of the spectrum to miss the diode array. This light loss is unlikely for the following reasons. First, the largest measured scatter in y-base values at room temperature is less than 30 microns (Hartig 1985). Second, the flattening was also seen in earlier data taken in June 84 (see Figures 5 and 6). Third, light loss cannot occur for the large 4.3 arcsec square A1 aperture and, therefore, cannot explain the increased time constant also seen for the A1 aperture. In June 1984, only red side data were obtained; and those data are not useful for linearity analysis, because a 50% neutral density filter was used instead of the 10% filter that was found necessary.

In an attempt to correct for the photocathode fatigue a model was used which allows the time constant to vary linearly above 51,000 counts. The resulting model computed for t is:

$$t = \begin{cases} 9.43 \times 10^{-6} \text{ sec} & y<51000 \\ 9.43 \times 10^{-6} + 2.568 \times 10^{-10} (y-51000) & y \geq 51000 \end{cases}$$

Figure 7 shows the results of this model as well as the case where t = 9.43 microsec for all count rates. If the fatigue effect is due to the limited current carry capacity of the photocathode substrate, then the results presented here may overestimate the importance of fatigue in the flight situation. The 2.0 and 4.3 arcsec apertures are taller than the 1.4 arcsec height of the diodes. Therefore, more current is drawn in the laboratory calibration with fully illuminated apertures than is drawn for the same count rate from a stellar point source.

The large scatter of the data for aperture C3 for rates around 60,000 counts per second in Figure 4 indicates that the non-linearity at higher count rates is diode dependent. This diode dependent behavior may be due to a pulse "pile up" at high count rates. Both noise pulses and pulses from photon events have a width and shape associated with them that may vary from channel to channel. As the count rate increases the pulses can build up and unpredictable results can occur. At these high count rates, changes to the discriminator levels will effect the linearity. As the true count rate increases above 300,000 counts/sec, the amount of scatter in observed count rates decreases due to increased saturation. All channels should saturate fully at the inverse of the dead time, which is an observed rate of about 100,000 counts/sec. In fact, the maximum observed rate is about 80,000. Despite the good repeatability of diode-to-diode variation at high count rates as shown in Figure 8, there are no plans to implement a diode dependent linearity correction at this time.

The final anomaly, the curved structure of the data between 30,000 and 50,000 counts/sec in Figure 3 can be attributed to an apparent spectral motion caused by high voltage setting and thermal effects over the four hour period required to take the data. Unlike the blue side, the spectral y-bases were not checked prior to data collection. As a result, the spectrum may not have been centered precisely on the diode array; and light loss of a few percent occured along the spectrum due to the small curvature induced by the imperfect magnetic focusing within the Digicon. The light loss in the smaller apertures is about 10 times less than the reduction of the count rates in C3 that is attributed to photocathode fatigue, as discussed above. A repeatability check of aperture C1 was taken during data collection. Figure 9 shows the ratio of two spectra taken approximately 2 hours apart. The low frequency variations in Figure 9 can be attributed to motion of the slightly curved

spectrum toward the edge of the diode array. Larger flux variations appear at the ends of the diode array, because the curvature effects are greatest there. In an attempt to improve results for the red side, the analysis was repeated using only the central 301 diodes. Figure 10 shows the new time contants versus observed count rate; and Figures 11 and 12 show a comparison of the model below 100,000 true counts/sec when using all diodes and only the center 301 diodes, respectively. A large improvement in the scatter is evident, while using the same time constant model. In Figure 12, the remaining deviation of the data from the model between 80,000 and 100,000 true counts/sec may be due to residual thermal drift effects that are present even at the center of the array.

## V. Error Analysis

Figures 13-15 show a plot of the error in the model for true count rates. The scatter in Figures 13 and 14 must be attributed to photocathode granularity, since the spectra do not fall exactly at the same locations on the cathode, and since the counting errors due to counting statistics are less than 1%. Therefore, the error in the non-linearity model below 80,000 counts/sec cannot be estimated from these plots. An alternate approach is to estimate the error in the time constant in Figure 1. A safe estimate is 0.5 microsec error on t. This would lead to the following errors in the non-linearity model.

| true count rate | observed count rate | error |
|---|---|---|
| 100 | 100 | .005 % |
| 1,000 | 990 | .05 % |
| 5,000 | 4,800 | .25 % |
| 10,000 | 9,100 | .5 % |
| 20,000 | 17,000 | 1.0 % |
| 30,000 | 23,000 | 1.5 % |
| 40,000 | 29,000 | 2.0 % |
| 80,000 | 46,000 | 4.0 % |

The data for the red detector is consistent with the blue detector up to 80,000 counts/sec. Above 80,000, the red-side errors can be estimated from Figures 14 and 15.

Red Side Only

| true count rate | observed count rate | error |
|---|---|---|
| 100,000 | 51,000 | 5 % |
| 150,000 | 57,000 | 25 % |
| 200,000 | 60,000 | 50 % |

If the increase in the time constant above 100,000 true counts/sec is due to photocathode fatigue, results for the red tube may not be applicable to the blue tube. The red tube studied here is not the flight tube, so these results must be verified in orbit, especially at high count rates.

## REFERENCE

Hartig, G. 1985, CAL/FOS-017, "Improvements in Filter/Grating Wheel Repeatability."

## FIGURE CAPTIONS

1. Computed time constant for the blue tube versus observed count rate.

2. Observed data over-plotted on the computed non-linearity model.

3. Computed time constant for the red tube versus observed count rate. The solid line is the computed model for the time constant.

4. Observed count rate for the red tube for all apertures with no filter as taken in August of 1984 on grating H57.

5. and 6. Comparison of the red tube C1 and C3 apertures for June 84 and August 84. Both sets are with no filter. The A1 data would have been shown, if that aperture had been observed in June 1984.

7. Observed count rate versus true count rate for the red tube. Over-plotted with a solid line is the computed non-linearity model. Upper solid line shows the non-linearity model, if the time constant does not change at high count rates.

8. Repeatability of the diode to diode variations for the red tube, aperture C3, from June 84 to August 84. The offset in mean level between the two observations is probably caused by small changes in the light source.

9. Ratio of the count rates for the red tube C1 (1 arcsec square) aperture taken approximately two hours apart (August 1984).

10. Same as Figure 3 and for the same time constant model. Only the central 301 diodes were used in analysis.

11. and 12. Comparison of the non-linearity model for t=9.43 microsec overplotted with the observed data for the red tube when all diodes are used and when only the central 301 diodes are used.

13. Per cent error of the observed true count rate versus the computed true count rate blue tube.

14. and 15. Same as 13, except for red tube.

Figure 1

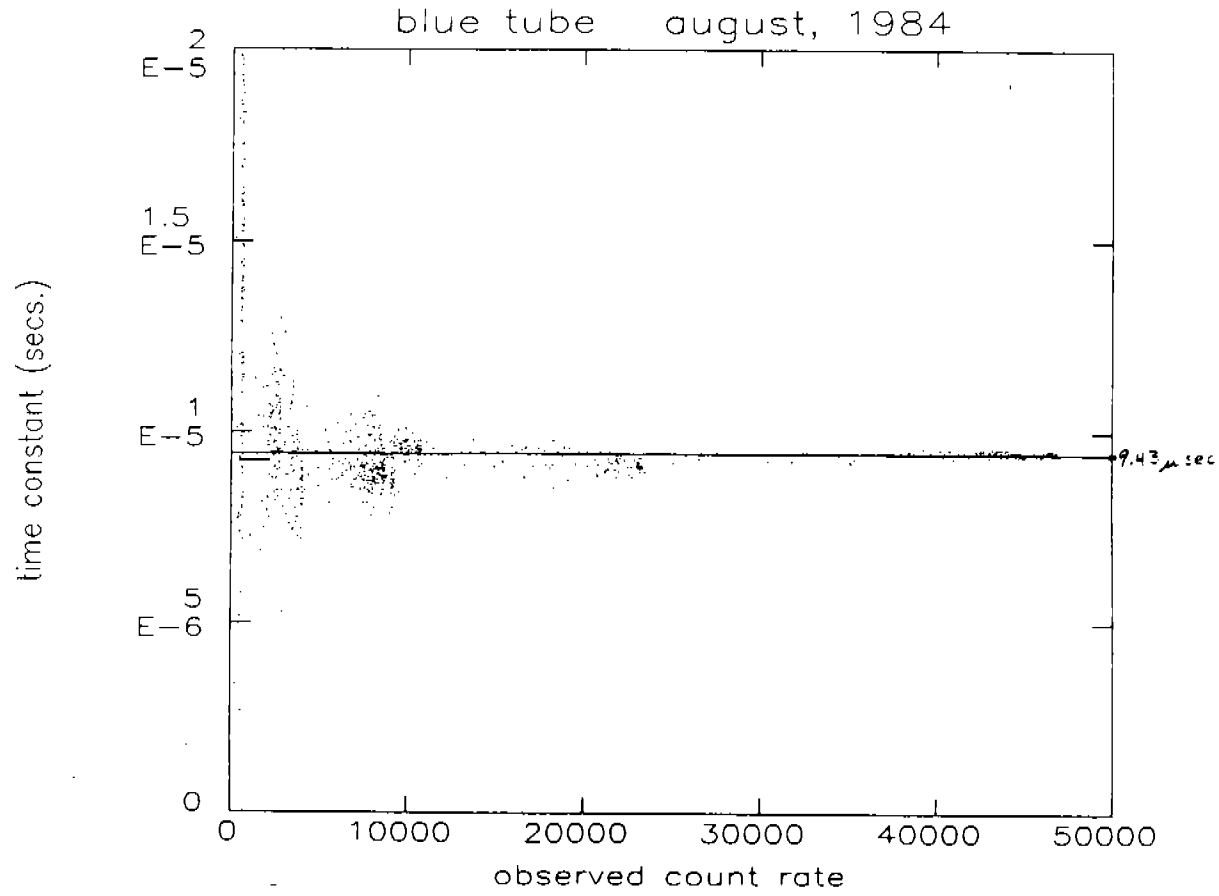


Figure 2:

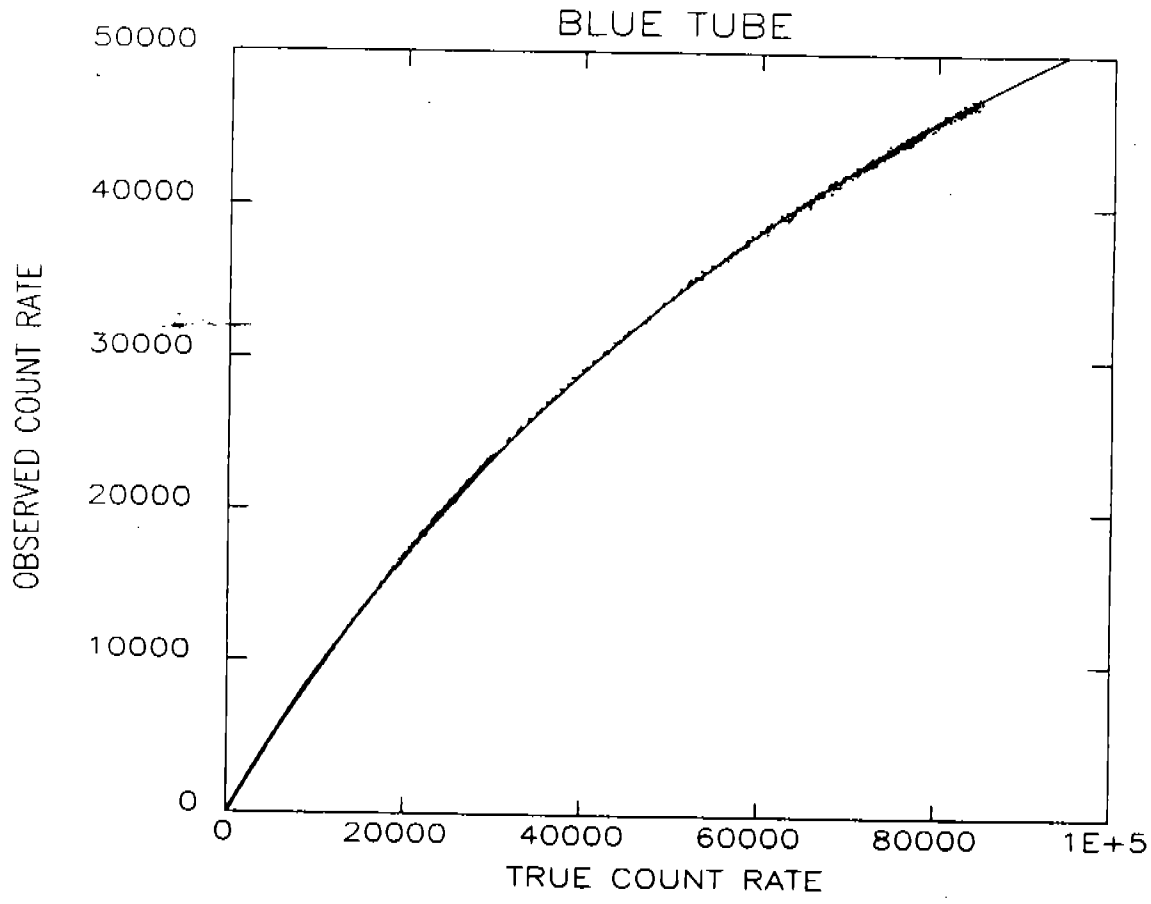

Figure 3:

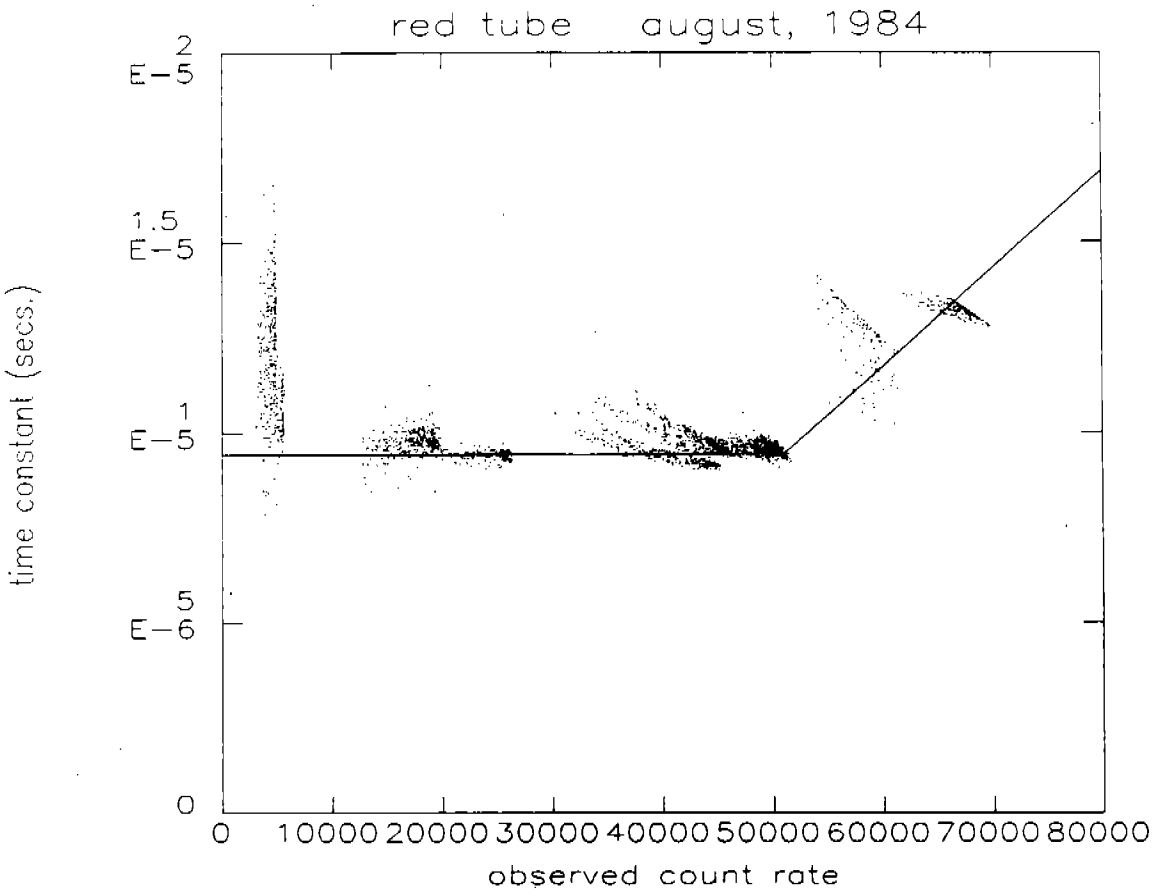


Figure 4

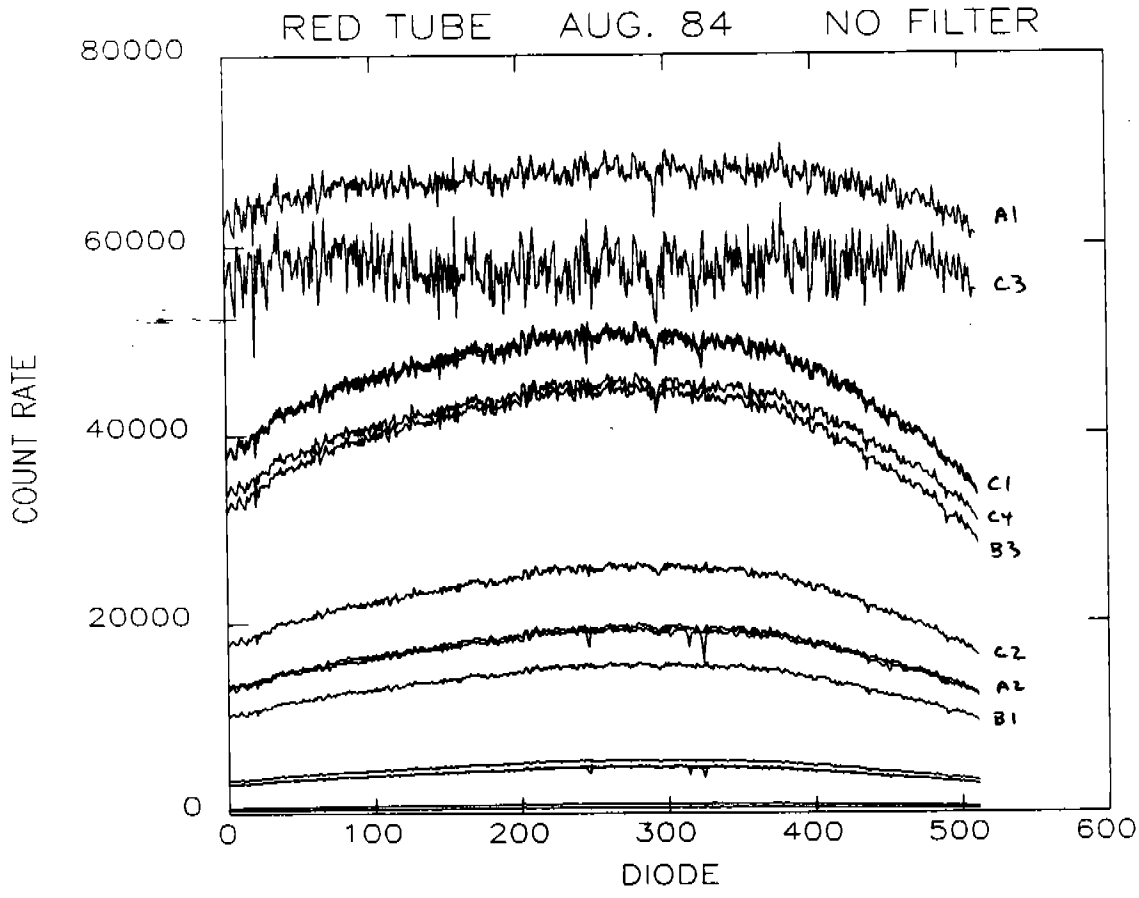

Figure 5

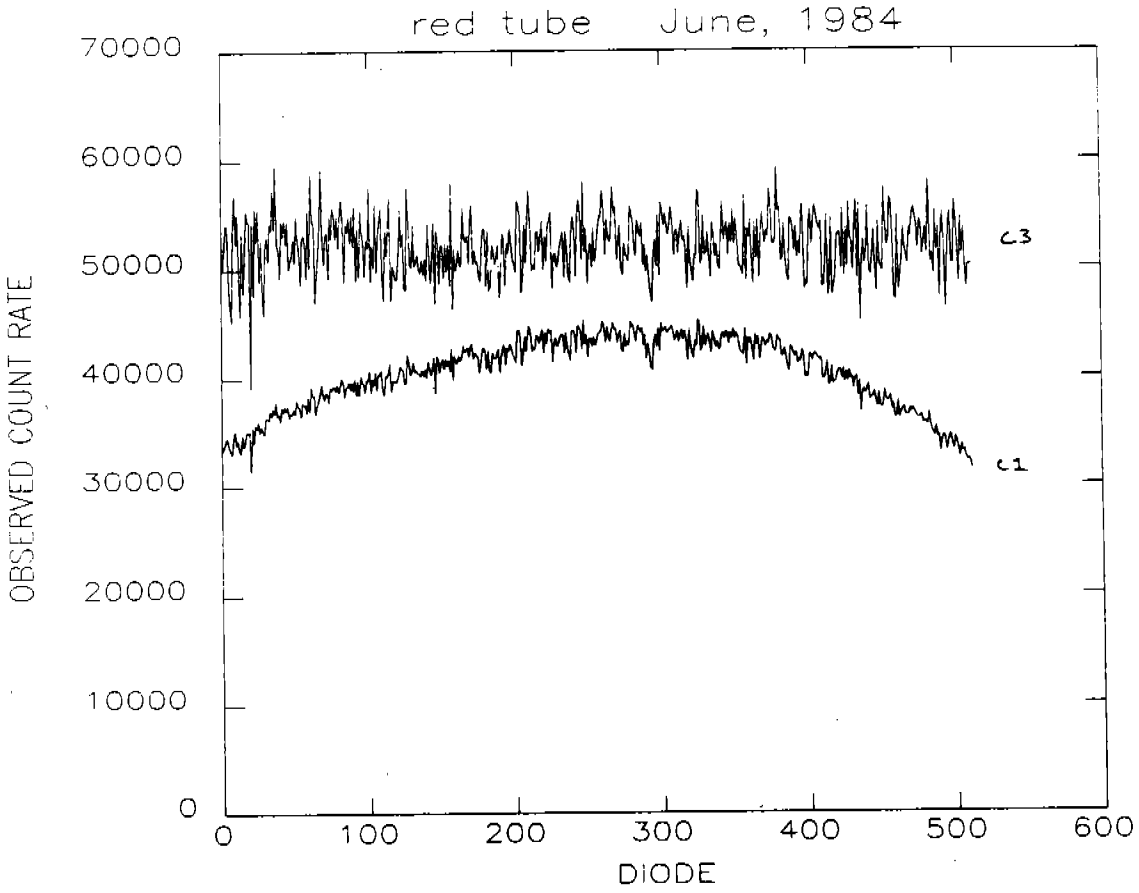


Figure 6

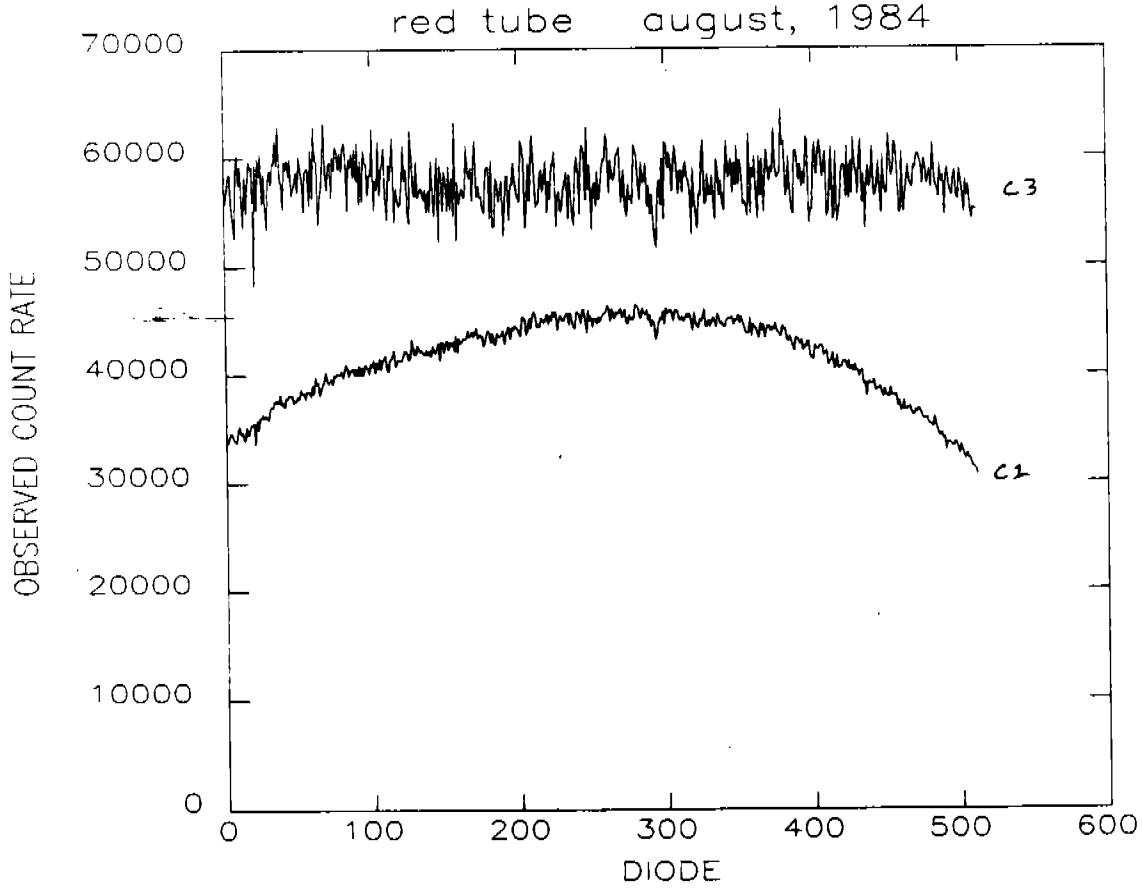

Figure 7

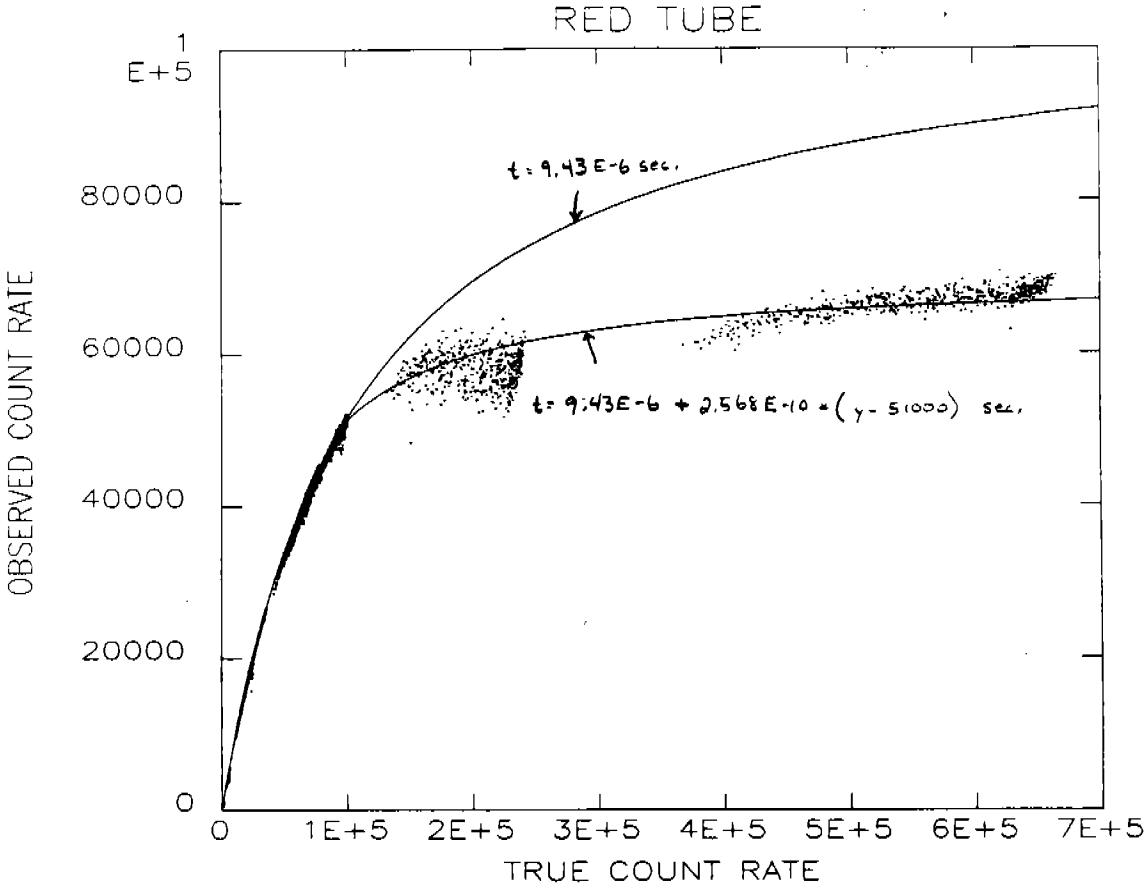


Figure 8

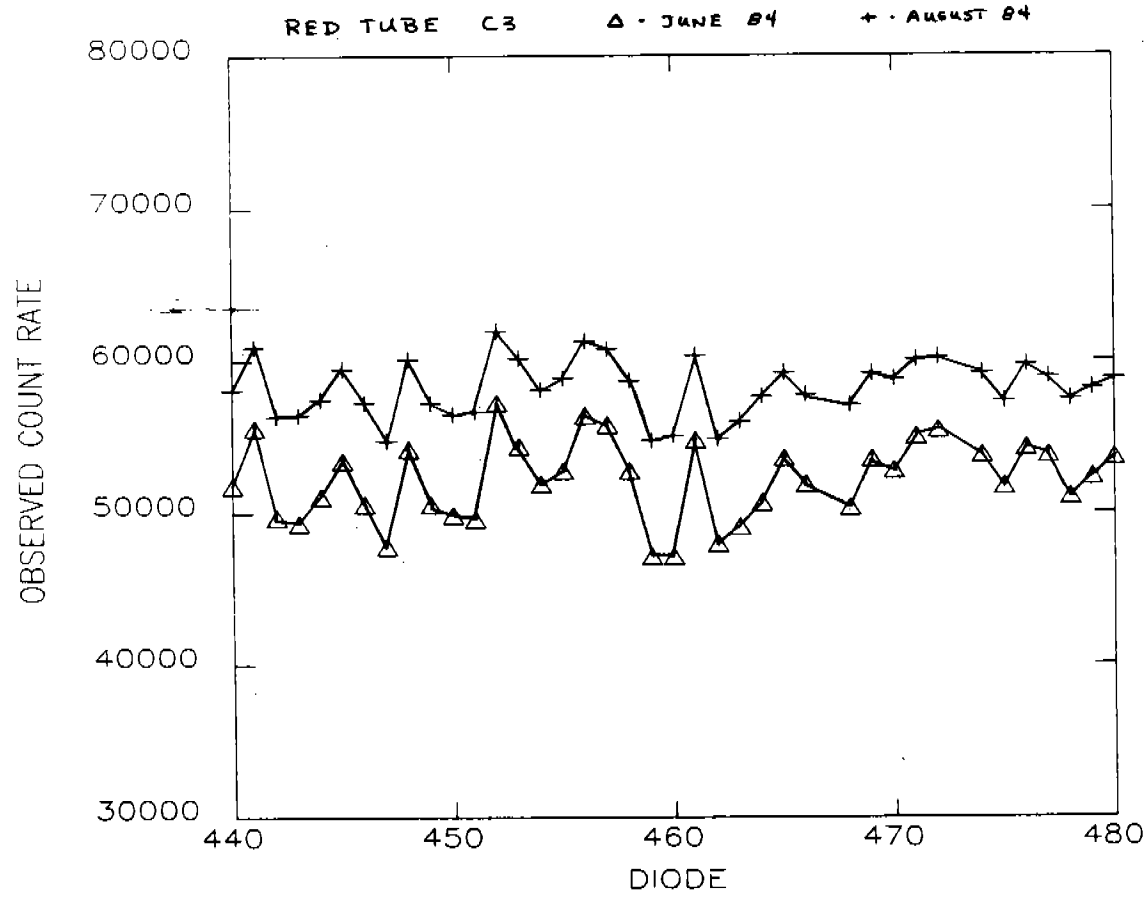

Figure 9

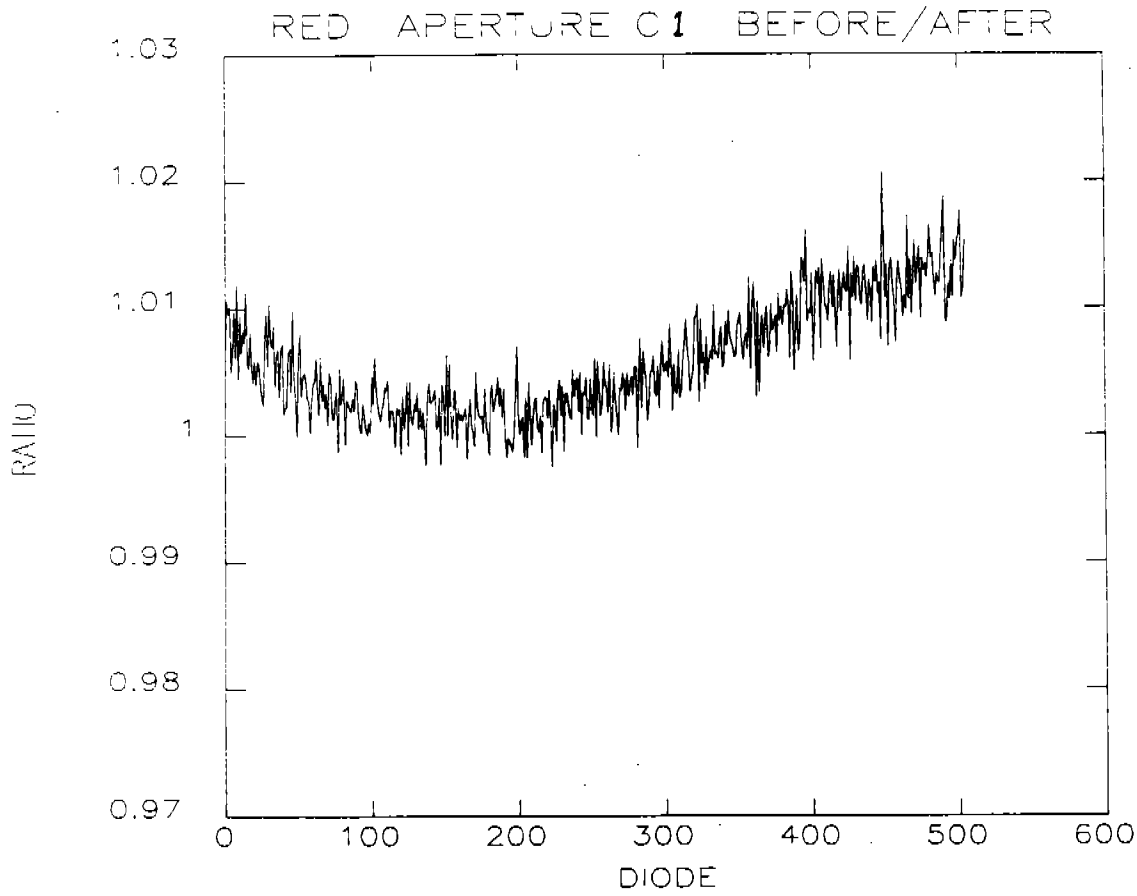


Figure 10

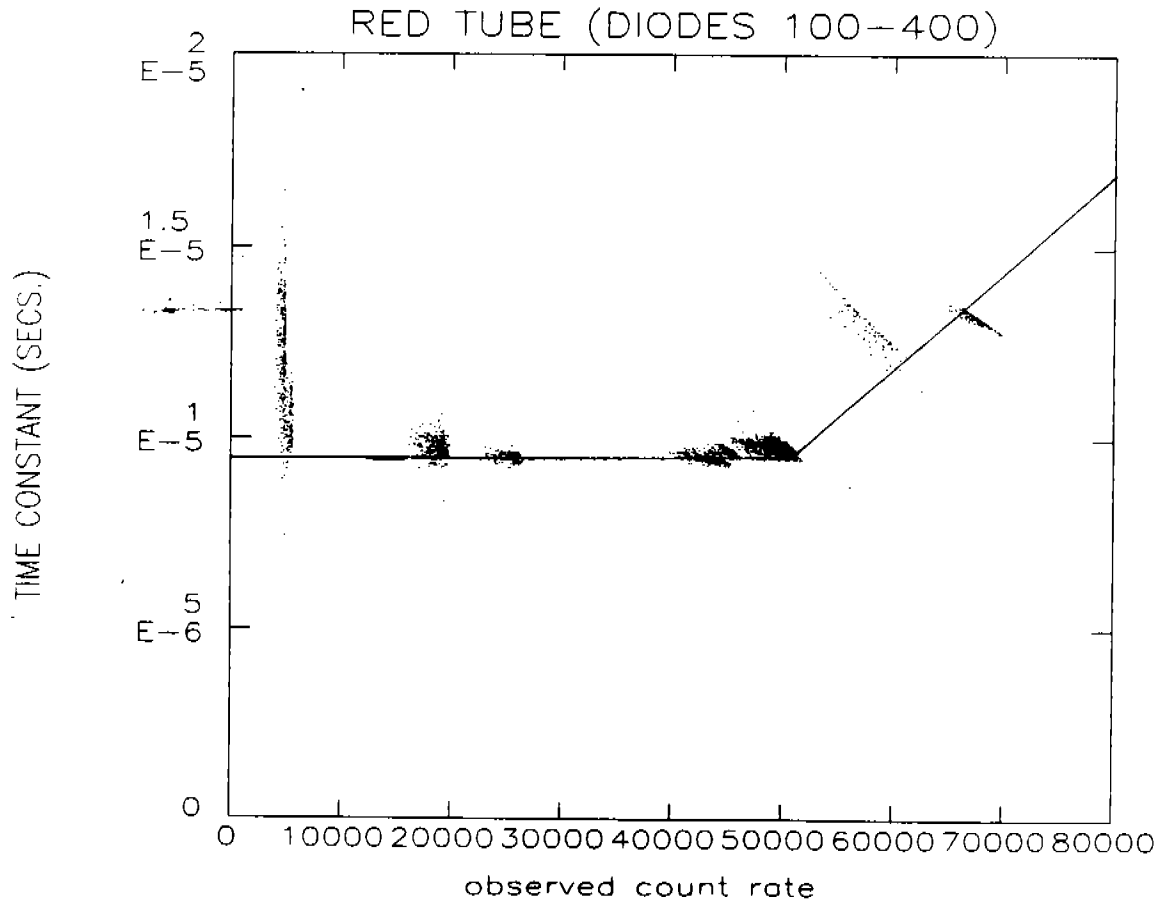

Figure 11

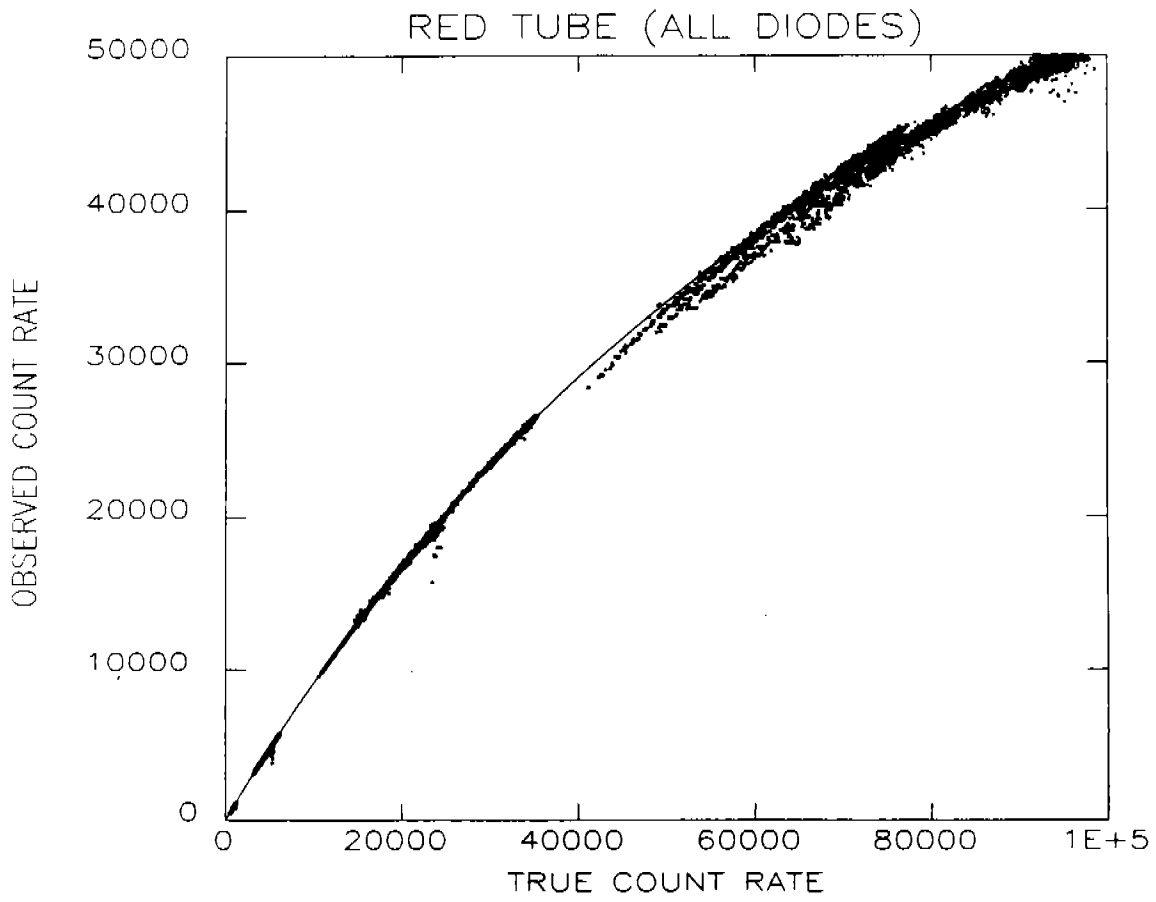


Figure 12

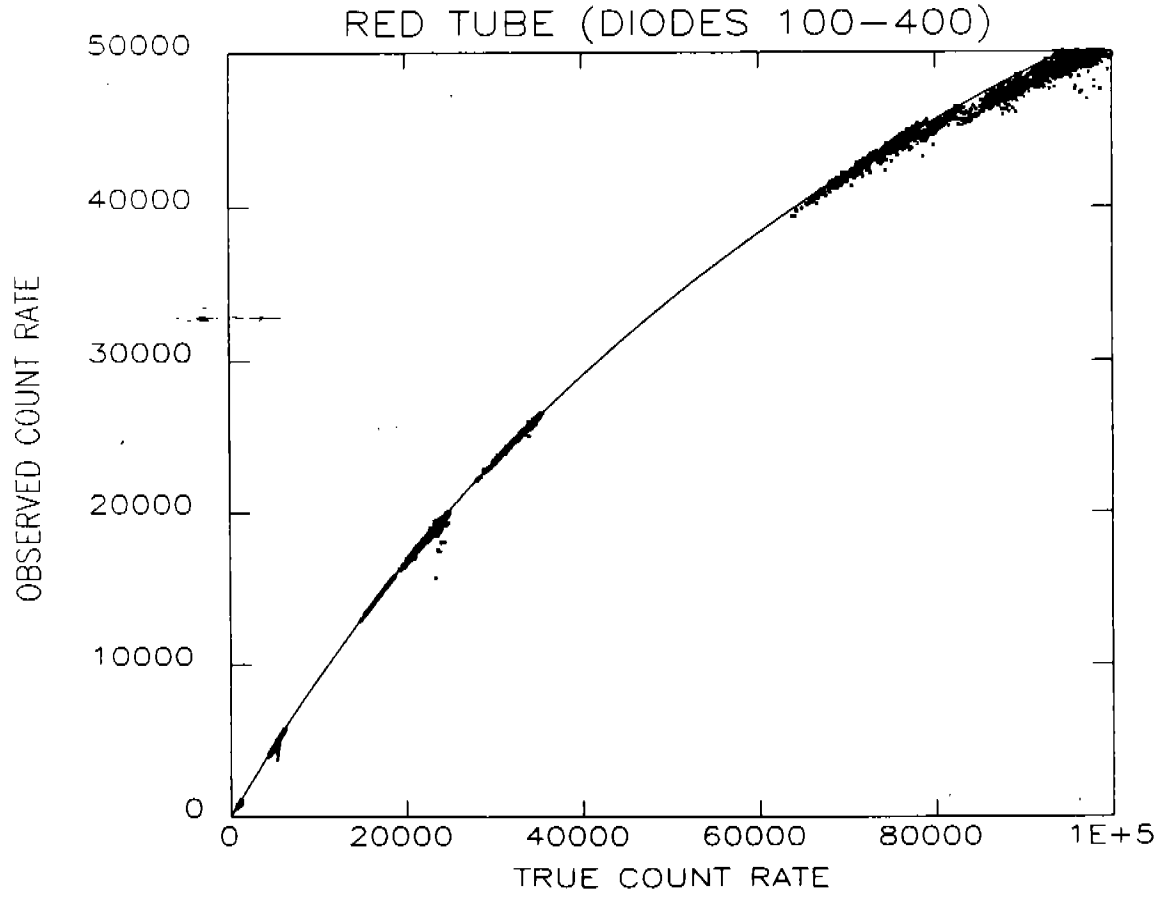

Figure 13

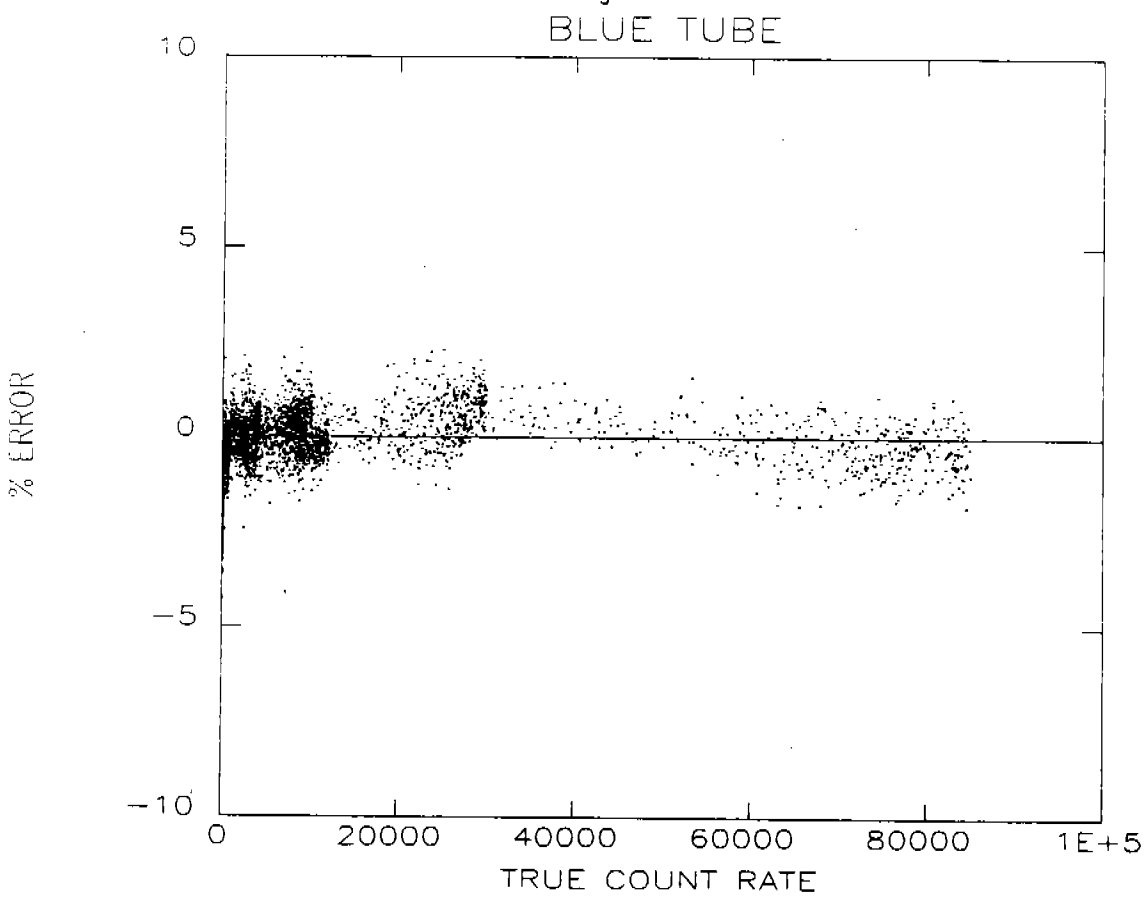


Figure 14

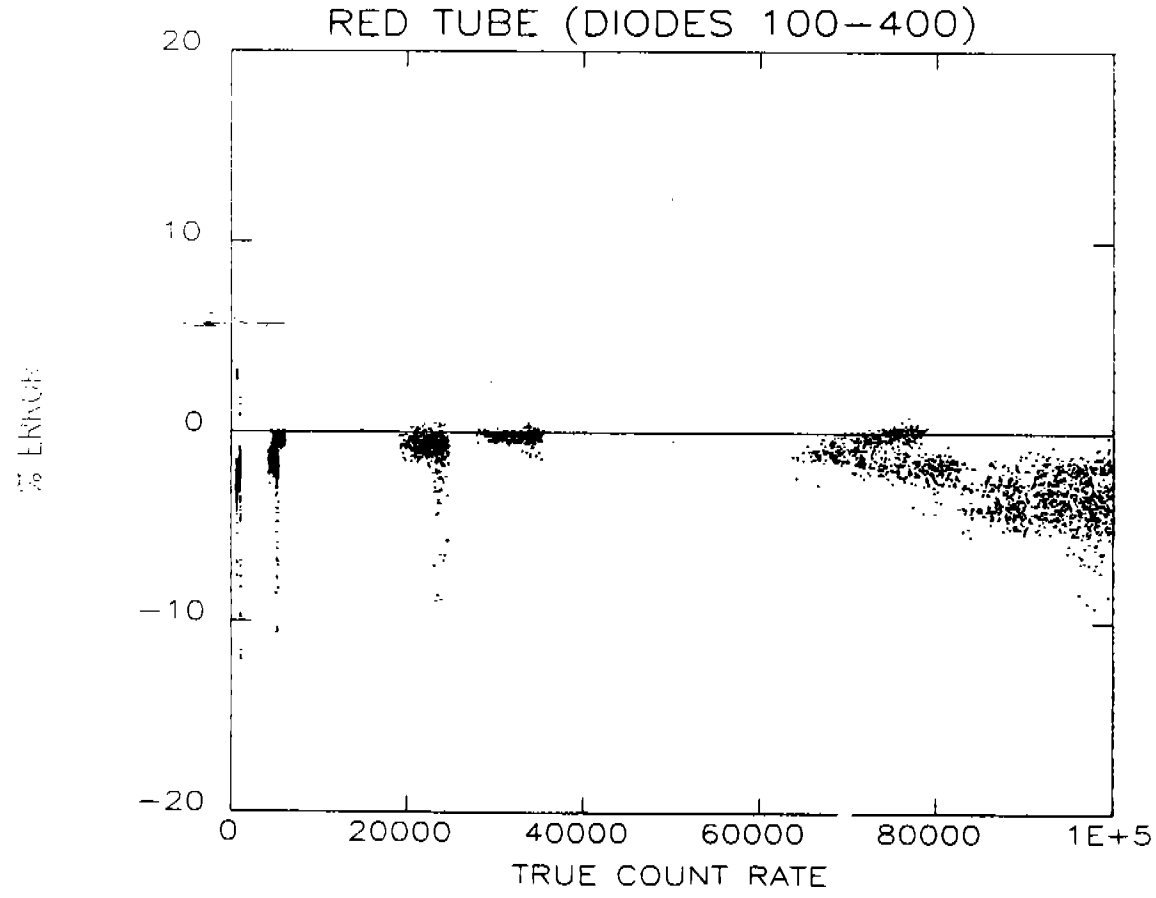

Figure 15

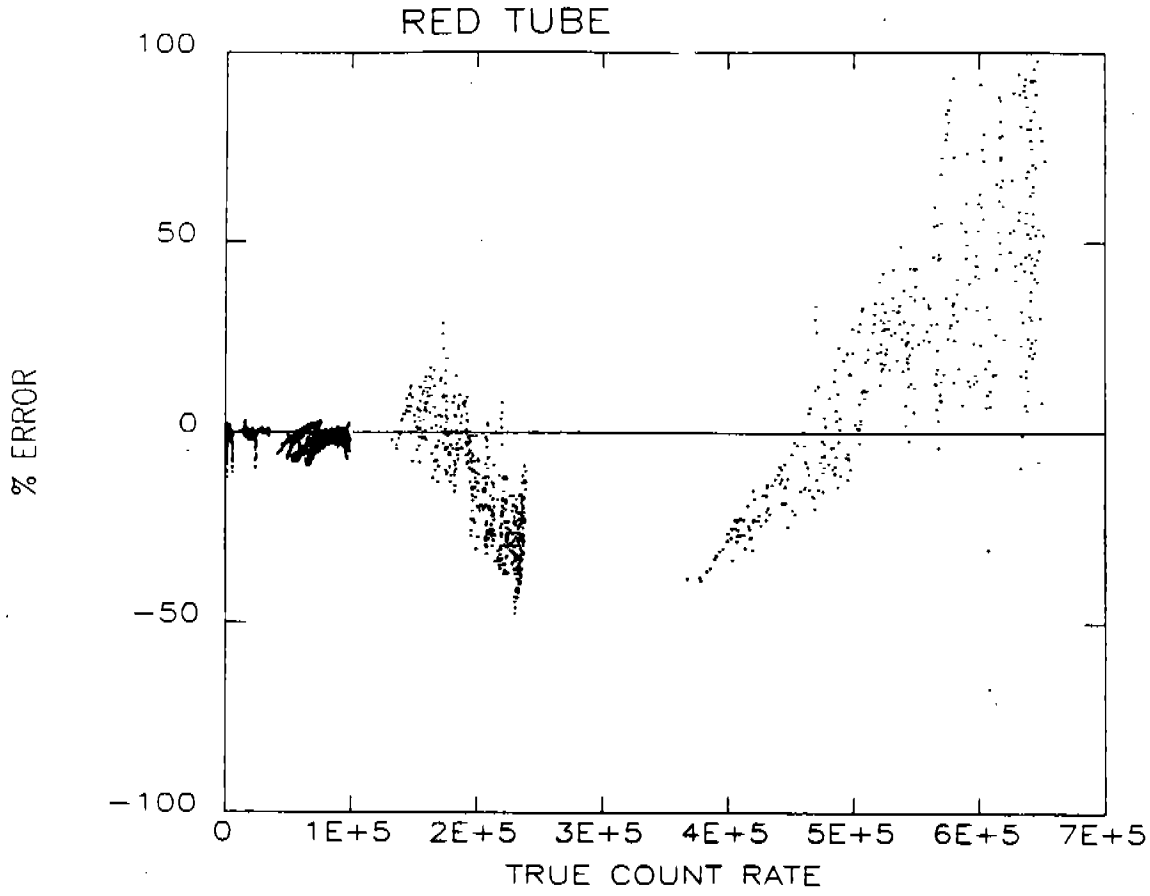
RED TUBE
100
50
0
−50
−100
% ERROR
0
1E+5
2E+5
3E+5
4E+5
5E+5
6E+5
7E+5
TRUE COUNT RATE